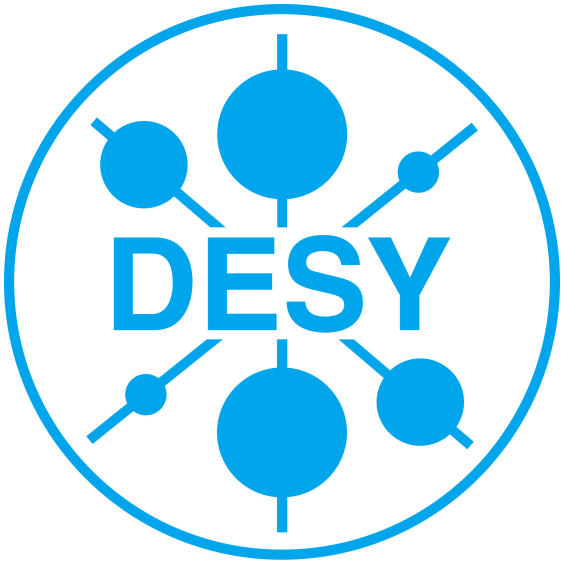

Studies on the AHCAL

Extraction of saturation curves from electron beam data

Christoph Jagfeld, Ludwig Maximilans Universität München, Germany

September 6, 2017

Abstract

With Silicon Photo Multipliers (SiPMs) it is possible to measure single photon radiation. Out of one incoming photon up to 10^6 electrons are created. Since they are small sized and easy to produce SiPMs are often used in particle detectors to read out scintillation light. For example SiPMs are used in the Analog Hadronic Calorimeter of the ILD detector. The saturation of the SiPMs must be understood, in order to analyze the resulting signal. Since the saturation of a large number of SiPMs needs to be determined SiPMs precisely, simpler methods of probing SiPMs are pursued. This report shows an attempt to extract the saturation effects directly out of electron beam data.

Contents

1. Introduction

Today elementary particles and their interactions are classified by the standard model. This has been proven quite successful in high energy experiments.However, this model is incomplete and not fully probe. For example it fails to explain the existence of dark matter and the connection of gravitation to other natural forces. The goal of particle physics is to probe and fully understand the standard model or find new physics beyond it.
In the standard model masses of gauge bosons are created through the coupling to the Higgs field. This process is not precisely probed yet. One of the main goals for future particle physics experiments is the measurement of the higgs coupling strength.
Currently the largest collider experiement is the LHC at CERN. It collides protons with a center of mass energy up to 14 TeV and probes "the Standard Modell at previously unreached energy scales"[1]. Since protons are composite particles only a randomly choosen center of mass energy is available for the collision.[1]
The International linear collider is designed to accelerate and collide positron and electrons. Because of the reduced hadronic background and the well-known initial state, a lepton collider would be highly favored for highest precision measurements of the higgs properties. To avoid energy loss due to synchroton radiation, the ILC will be a linear accelerator with a total length of 31 km and center of mass energies of 250 GeV up to 500 GeV (see figure 1).
Two different detectors, the International Large Detector (ILD) and the Silicon Detector (SiD) will be placed at the interaction point in the middle of the accelerator. The detectors could be pulled in and out of the interaction region.
ILD will be built up similar to other collision experiments. In the middle of the detector a tracking system will be installed. This will be surrounded by an electromagnetic calorimeter and an Analog Hadronic Calorimeter (AHCAL). Since the AHCAL is a highly granular calorimeter with many read out channels it is well suited for Particle Flow Algorithms.
In this report studies are performed on the AHCAL.

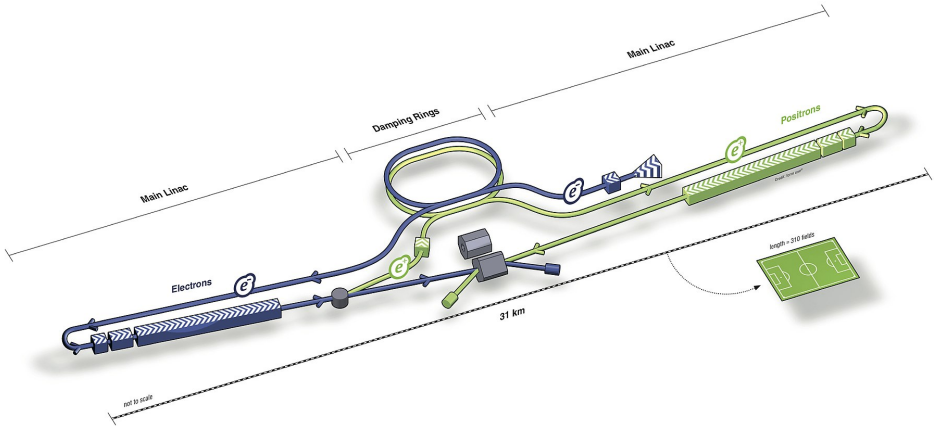

Figure 1: Schematic figure of the international linear collider; taken from [2]

2. Construction of AHCAL

2.1. Energy loss in matter

The following is a summary of energy loss mechanisms in matter. Further details can be found in REF. [1].
An electron traversing through matter gets deflected on nuclei or electric- and magnetic fields and thus accelerated. When accelerated, charged particles lose energy due to bremsstrahlung. After traversing the radiation length X_0 through matter, the remaining kinetic energy of the electron is reduced to $1/e$ of its initial energy.

$$X_0 \sim \frac{A}{\sqrt{Z}(Z+1)} \tag{1}$$

Where A is the mass number and Z the atomic number
If the energy of a photon is higher than the production threshold $E_\gamma \geq 2m_e$ of an electron-positron pair, the photon is loosing its energy due to pair production.
When a high energetic electron enters dense matter, both bremsstrahlung and pair production leads to energy loss.
At first bremsstrahlung is dominant. The photons again produce electron positron pairs, which loose further energy due to bremsstrahlung (see figure 2). An electromagnetic shower is created.

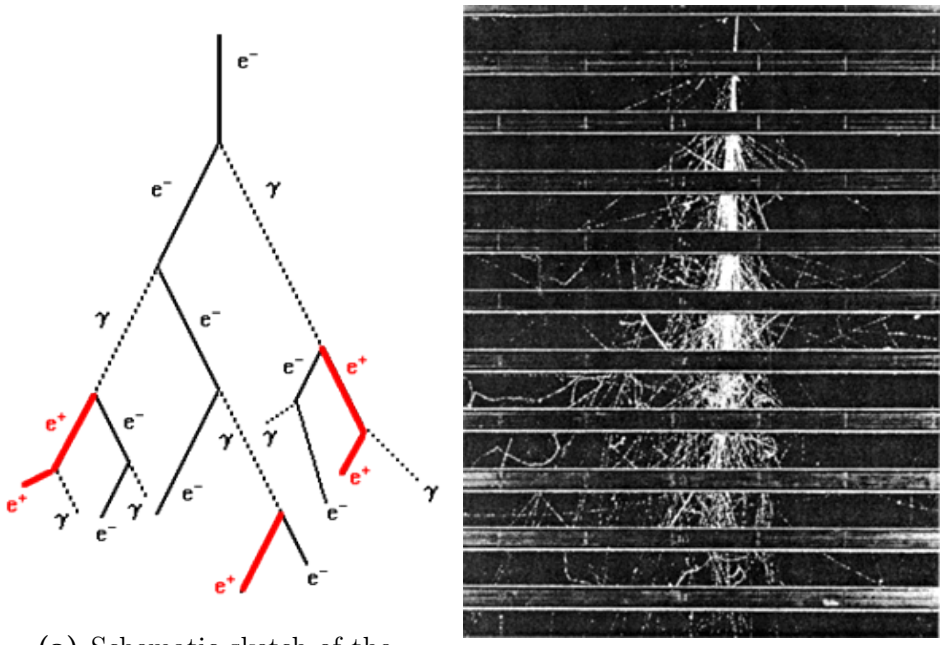

(a) Schematic sketch of the development of electromagnetic shower.

(b) Picture of an electromagnetic shower.

Figure 2: Pictures are taken from [3].

The amount of particles is roughly doubled within X_0. At the critical energy E_c, the energy loss due to bremsstrahlung and ionization are equal in one branch the electromagnetic shower will stop for that specific branch
The maximum of particles in the shower is found at X_{max}:

$$\frac{X_{max}}{X_0} = ln(N) - 0.5 \tag{2}$$

Where $N = E_0/E_c$ is the number of particles generated in the shower. Due to high energy densities in an electromagnetic shower which leas to saturation, the AHCAL is probed in an electron beam. In the AHCAL the electromagnetic shower created by a charged particle or photon is captured and measured.

2.2. Construction of the AHCAL

The AHCAL design consists of alternating active scintillator and heavy absorbing steel layers. In the absorbing layer the electrons gets decelerated and a shower is created.
In the active layer the transversing particles creates scintillation light. The signal is read out by silicon photo multipliers(SiPMs).
Following studies were performed with a prototype of AHCAL. This prototype is constructed out of 17 absorbing layers. 15 out of 16 slots in between were equipped with active layers. 2160 3cm × 3cm × 0.3cm plastic scintillator tiles are used for active layers (figure 3), equaly split up between them. The SiPMs are soldered to the PCB and the wrapped tiles are glued to the PCB. All SiPMs are read out using the same electronics. The number of pixels for the used SiPMs can be found in the appendix in table 1.

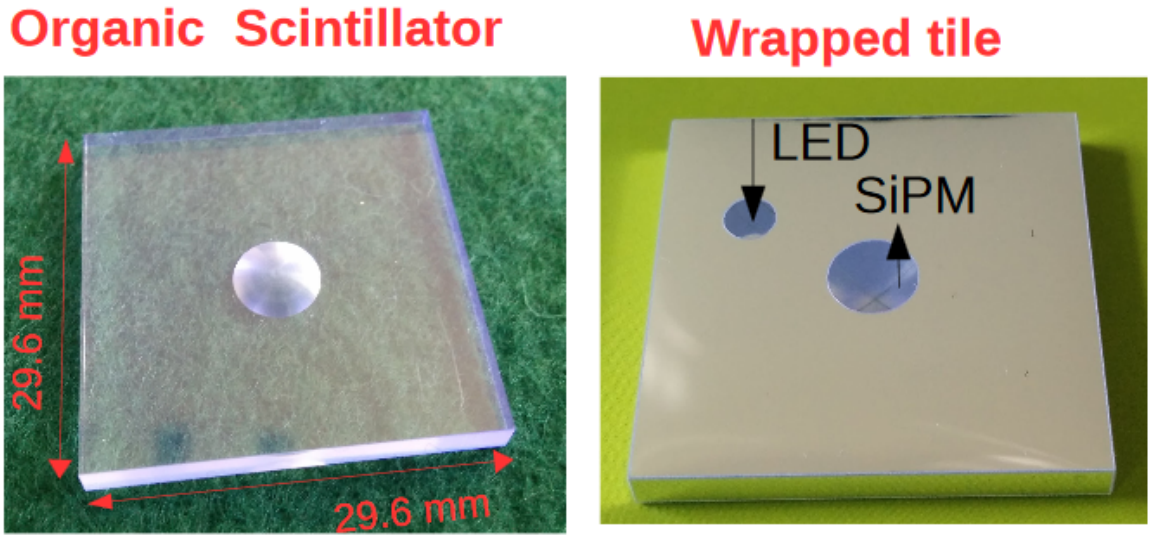

Figure 3: Scintillator tile.
The SiPM will be glued in the middle. To reduce cross talk between the tiles by photons leaving one tile and entering the next tile the SiPMs are wraped. Taken from [4]

2.3. Silicon Photo Multipliers (SiPMs)

SiPMs are semiconductor devices. Since they are smaller, easier to produce and cheaper they are highly favored to be used for the AHCAL instead of classic photo multiplier tubes.
SiPMs consists out of a matrix of light sensitive avalanche photo diodes, placed on a few mm^2. These pn-diodes are operated in reverse bias. A single incoming photon is sufficient to create an electron hole pair in the depletion region. Due to a large external voltage the electron gets accelerated and causes an electron avalanche. After a pixel had been fired, it needs some time to recover. During that time no events can be detected. The number of incoming photons can be reconstructed out of the number of fired pixels. Since the number of pixels is finite, the relation between measured number of incoming photons and the number of actual incoming photons is non linear. Rather the dependence follows a saturation curve. The curve is saturated. This curve can be described by equation 3.

$$\langle n \rangle = m(1 - e^{\gamma/m}) \tag{3}$$

Where n is the number of fired pixels and γ the number of incoming photons.
An exemplary saturation curve of a SiPM, obtained by simulation, can be seen in figure 4. If a pixel recovers during an event it can fire twice. Therefore the measured number of fired pixels then is larger than the actual number of pixels in the SiPM.
To consider the saturation of SiPMs for the analysis the number of effective pixels is needed. In the following different methods for trying to extract the effective number of pixels will be described.

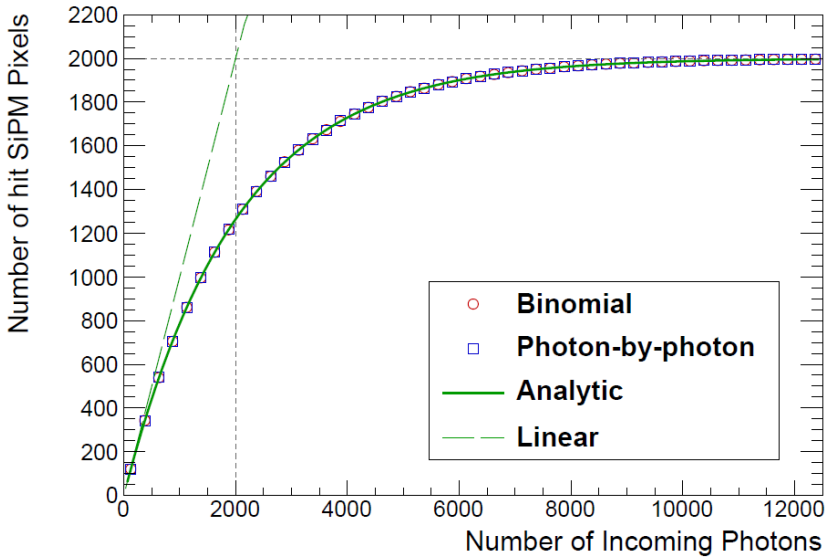

Figure 4: Simulated saturation curve of a SiPM with 2000 effective pixels.
The number of fired pixels does not exceed the number of effective pixels. Taken from [1]

3. Reconstruction of the number of incoming photons

For each scintilator tile the measured deposited energy E_{hit} is reconstructed. This number is proportional to the number of fired SiPM pixels.

$$n = LY \times E_{hit} \tag{4}$$

Where n is the number of fired pixels and LY the Light Yield. $LY = 23.3$.
The Light Yield is the number of fired pixels for a minimal ionizing particle (MIP) crossing the scintillator tile. As the goal is to observe saturation effects the tile which most likely shows such effects is chosen. It is assumed that the probability to see saturation is highest on the tile which is hit by the most photons and thus most of the energy is deposited (see figure 5). This tile will be called target tile.

The mean value of the beam energy equals to the mean value of the sum over the energies deposited on all the tiles. In the following the sum of E_{hit} over all tiles will be named energy sum E_{sum}.

$$E_{sum} = (E_{hit})_{target\ tile} + \sum_{other\ tiles} E_{hit} \tag{5}$$

One assumes that the mean value of the energy sum $\langle E_{sum} \rangle$ for lower deposited energies E_{hit} is not affected by saturation effects.
By setting equation 5 equal to $\langle E_{sum} \rangle$ one can calculate the hit energy of the target tile without saturation effects (equation 6).

$$\langle E_{sum} \rangle = (E_{hit})^{w/o\ saturation}_{target\ tile} + \sum_{other\ tiles} E_{hit} \tag{6}$$

This equation can be solved for $(E_{hit})^{w/o\ saturation}_{target\ tile}$ (equation 7). Since it is assumed that the target tile is affected by saturation effects, this value is proportional to the number of incoming photons.

$$(E_{hit})^{w/o\ saturation}_{target\ tile} = \langle E_{sum} \rangle - \sum_{other\ tiles} E_{hit} = \langle E_{sum} \rangle - (E_{sum} - (E_{hit})_{target\ tile}) \tag{7}$$

In the following $\langle E_{sum} \rangle$ is called reference energy. In ideal case the calculated hit energy $(E_{hit})^{w/o\ saturation}_{target\ tile}$ can be assumed as the actual hit energy.
The reference energy must be estimated very precise such that it includes as little saturation effects as possible.

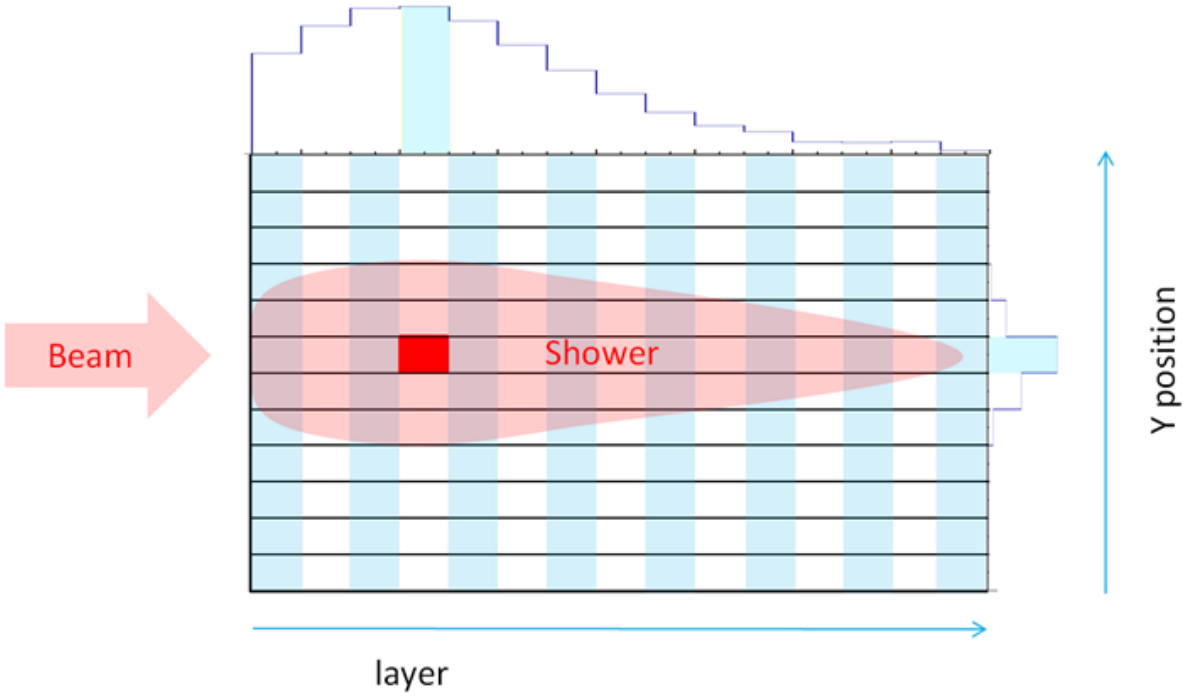

Figure 5: Determination of the hottest tile.
The light red shows the development of the shower inside the different layers and tiles in y-position. The graphs on the top/side shows the statistics of the events in the corresponding direction.
The marked tile is the tile where most events takes place (target tile).

4. Analysis

The data for the runs with beam energies up to 5GeV, were taken in July 2016 at the DESY electron test beam using the prototype described in section 2.2. The 10GeV and 20GeV data had been taken in May 2017 at the CERN SPS test beam facility with electron beams using the same prototype.

4.1. Event selection

Since we are interested in the saturation of one single SiPM the tile where most events take place is considered. Exemplary for all the different beam energies the distribution of the shower in the AHCAL for 1GeV is shown in figure 6. The selected tiles for all beam energies are shown in the appendix in table 2.

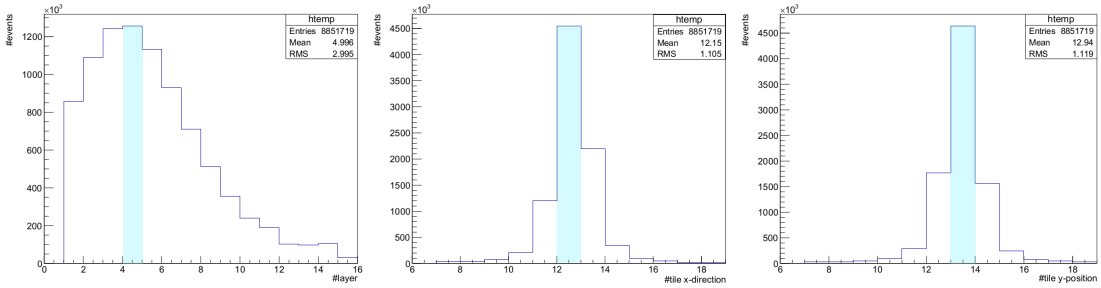

(a) Distribution of hits on the different layer.

(b) Distribution of hits on the different x positions.

(c) Distribution of hits on the different y positions.

Figure 6: Distribution of the hits on different position in the AHCAL for 1GeV. The tile with the most statistics, which is marked in blue, will be selected.

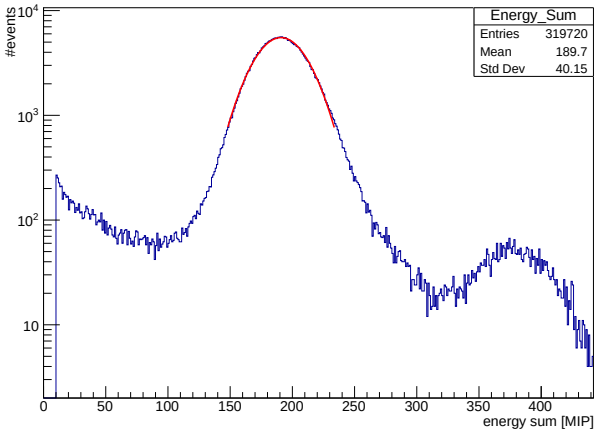

Figure 7: Energy sum distribution for 4 GeV beam data.
Events smaller than 10 MIP are considered as noise and are cut off.
Only events in the range $+/-2\sigma$ are taken into account to get rid of other unwanted events like the two electrons hit peak between 350MIP and 400MIP

A huge number of events is detected with energies below 10MIP. Since the energy of that events is much smaller than the beam energy, these events are considered as noise and are cut of (figure 7). Further on one only consider events in the region of 2σ around the mean value of the Gaussian shape spectrum of the energy sum, to neglect unwanted events like events that probably contain a two electrons peak at 380 MIP (figure 7).
At last only events are taken for the studies, where hit target tile is in the center of of gravity of the beam.

4.1.1. Results

In figure 8 the measured hit energy is plotted against the calculated hit energy. Each point is determined by using the mean value of the measured hit energy for each bin. The corresponding energy $(E_{hit})^{w/o\ saturation}_{target\ tile}$ is been calculated for each bin width. The bin widths are shown in table 2.
As in figure 8, the different beam energies do not line up on one smooth curve. The calculated curves show big deviations from the reference saturation curves which are expected for these energies.
This is a clear hint that the chosen reference energy has to be replaced, since there is a strong correlation between the energy sum and the hit energy (figure 11). For this plot the corresponding energy sum is determined for each slice of measured hit energy.
In the following two different approaches are described to find a suited reference energy.

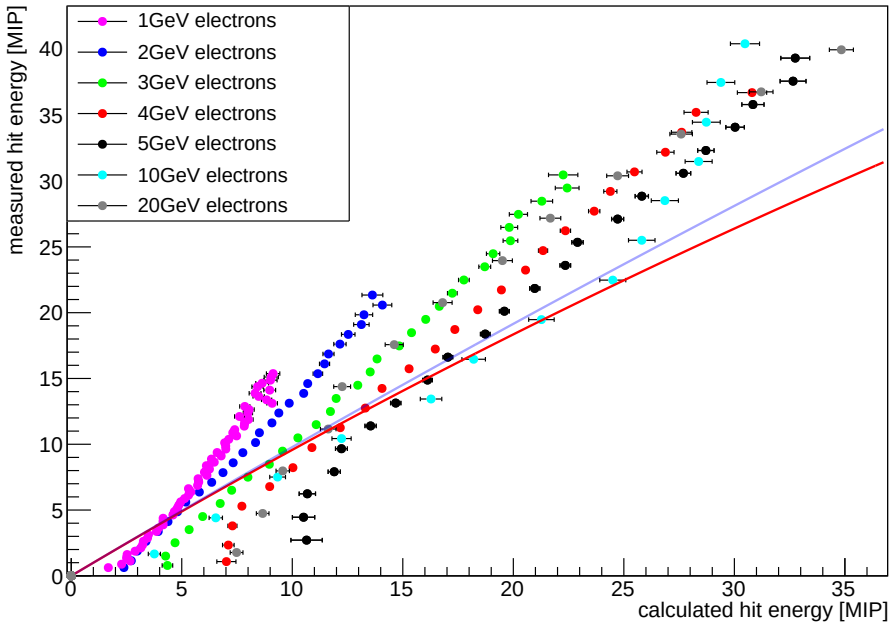

Figure 8: Correlation between calculated and measured hit energy for different beam energies. the blue and blue line are the saturation curves for:
blue: effective number of pixels = 2 × number of pixels
red: effective number of pixels = number of pixels

4.2. Selection of the correct reference energy

Since the energy sum is depending on the measured hit energy (figure 11),it is assumed that is a cause for the difference of the curves from the reference curve.

4.2.1. Sliced energy sum

The easiest way to take care of that effect is to use the corresponding value of the energy sum for each measured hit energy bin instead of the overall mean value of the energy sum. By using that value the measured hit energy gets closer to the expected saturation function, but the fluctuation of the calculated hit energy is still large (figure 9a). The corresponding graph for all beam energies is shown in the appendix in figure 13.

The target tile is not necessarily the tile with the most deposited energy. To minimize the fluctuations only events with maximum energy deposition on the target tile are used. Though this leads to shrinking of the statistics and stronger correlation between E_{sum} and E_{hit} (figure 11, blue curve) the values of the different beam energies form a smooth curve (figure 9b). However, no saturation is observed at all. The graph is linear. This is a clear hint that the saturation effect is already corrected in the determination of the mean energy sum in slices of E_{hit} in this sample. Therefor the mean value of the sliced energy sum can not be used as a reference energy neither.

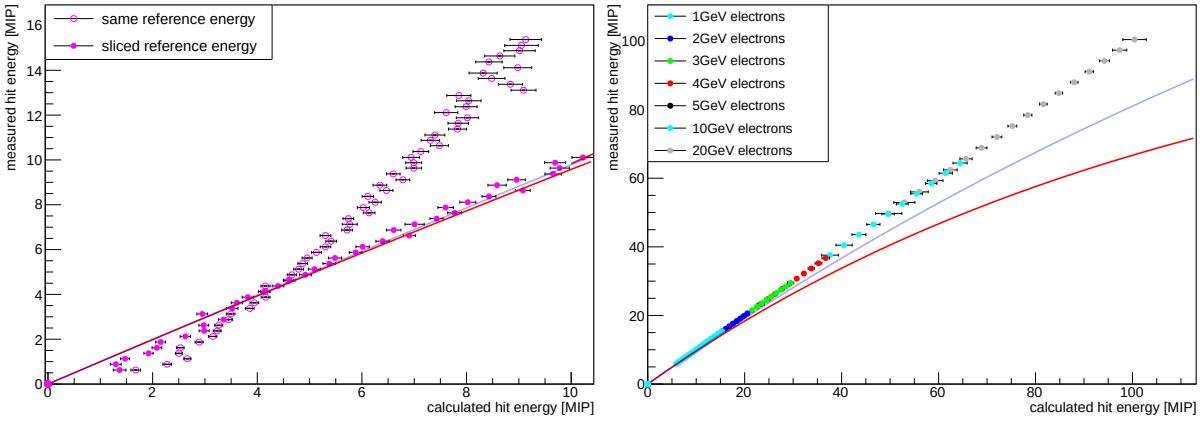

(a) Correlation between the measured hit energy and calculated hit energy for 1GeV beam data.
• : sliced mean energy sum as reference energy
◦ : overall mean energy sum as reference energy

(b) Only events with maximum energy deposition on target tile are used. The curves fit together.
The lines are the saturation curves for:
blue: # effective pixels = 2 × # pixels
red: # effective pixels = # pixels

Figure 9: Correlation between calculated and measured hit energy. As reference energy the Sliced energy sum is used. In both plats no saturation is observed.

4.2.2. Extrapolated energy sum as reference energy

The saturation of the SiPMs increases with increasing hit energy. Therefore one can assume that for low hit energies (for 1GeV: E_{hit} between 2 and 6 MIP) the corresponding energy sum is barely affected by saturation effects. By fitting a logarithmic function (equation 8) to the correlation curve of E_{sum} vs. E_{hit} in that energy range, values for E_{sum} at higher E_{hit} can be determined by extrapolation.

$$E_{sum} = a\ log(b\ E_{hit} + c) + d \tag{8}$$

In this case E_{hit} is the energy deposited on the target tile if it is maximum in that event. The resulting energy sum is less affected by saturation and can be used as a new reference energy in equation 7.
For 1 GeV beam energy the graph is shifted towards higher calculated hit energy values. and the fluctuation increased (figure 10).

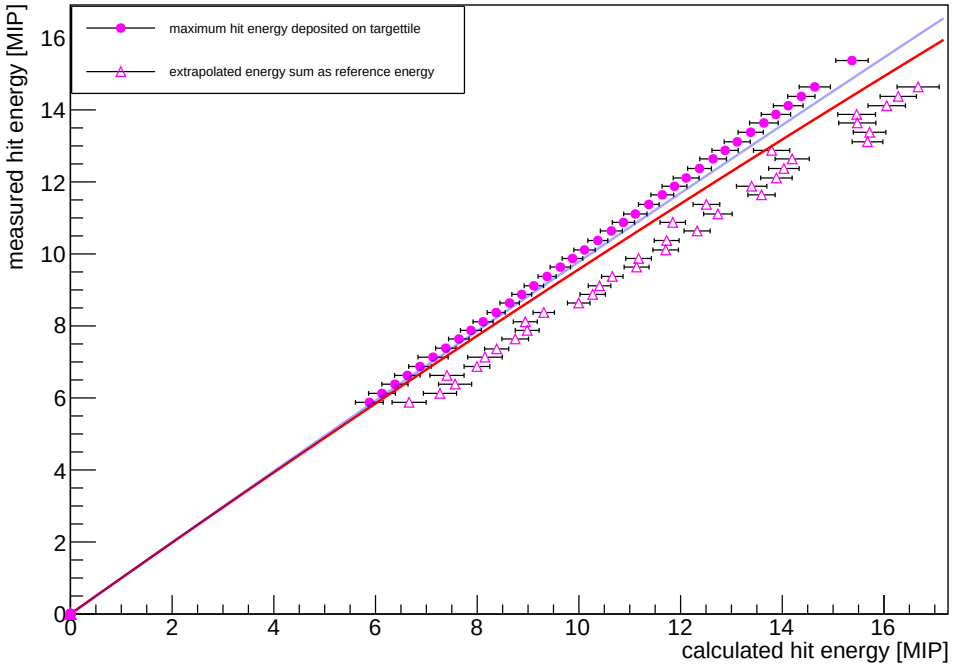

Figure 10: Saturation curves for 1 GeV:
• : target tile if maximum energy is deposited on it
△ : extrapolated energy sum as reference energy

Unfortunately this process only makes sense for low hit energies. Since the statistics for higher beam energies is too low in the low hit energy region, this method only works for low beam energies and graphs from different beam energies do not merge in one single smooth curve (appendix figure 14a). Only for 5 GeV the curve is close to the reference saturation curve. For 1Gev - 4GeV the deviations are still big.

4.2.3. Considering neighbor tiles

The Moliere radius of the electromagnetic shower in the absorbing material is $R_m = 1.72\ cm$. However, the tile size is $3 \times 3\ cm^2$, so that not the whole shower is trapped by the target tile. By calculating a cluster hit energy $E_{hit}^{cluster}$ for the target tile and its neighbor tiles, equation 9is taken into account. The cluster hit energy is better suited to determine the correlation between E_{sum} Vs E_{hit} more precise.

$$E_{hit}^{cluster} = E_{hit}^{target\ tile} + \sum_{neighbor\ \ tiles} E_{hit} \tag{9}$$

From the correlation curve of energy sum and cluster hit energy (figure 11, green curve) one can extrapolate values for an unsaturated energy sum, as described in section 4.2.2.

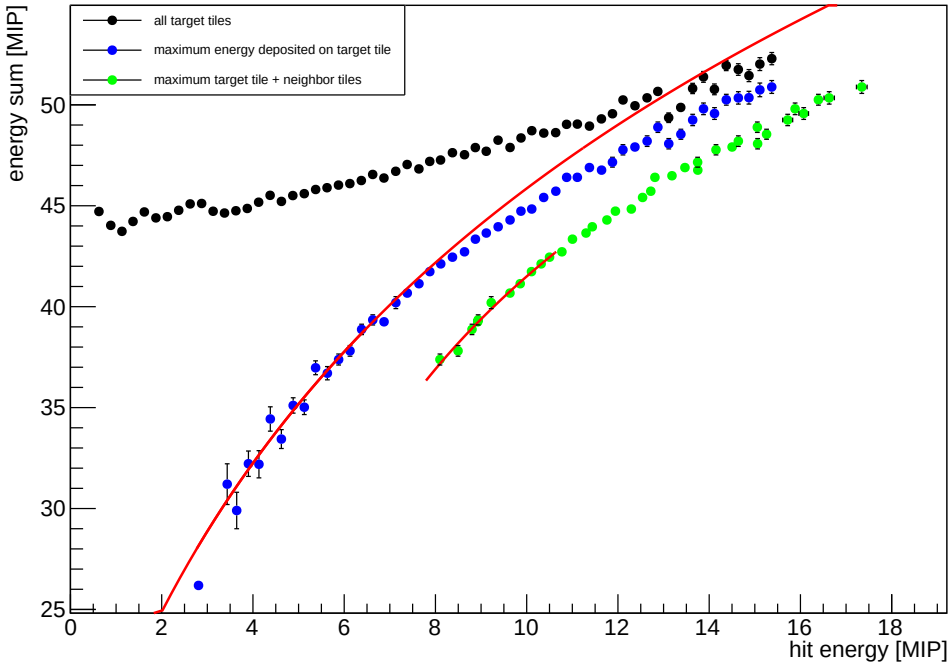

Figure 11: Correlation between the measured hit energy and energy sum for 1GeV beam data.
blue: only events when maximum energy is deposited on target tile
black: all events where energy is deposited on the target tile
green: all events where energy is deposited on the target tile and using cluster energy as hit energy
The red lines are the fitted logarithmic functions

This extrapolated energy sum can be used as a new reference energy in equation 7. The corresponding saturation curve can be seen in figure 12. Like in section 4.2.2 this method can only be used for small beam energies. However, no saturation is observed.

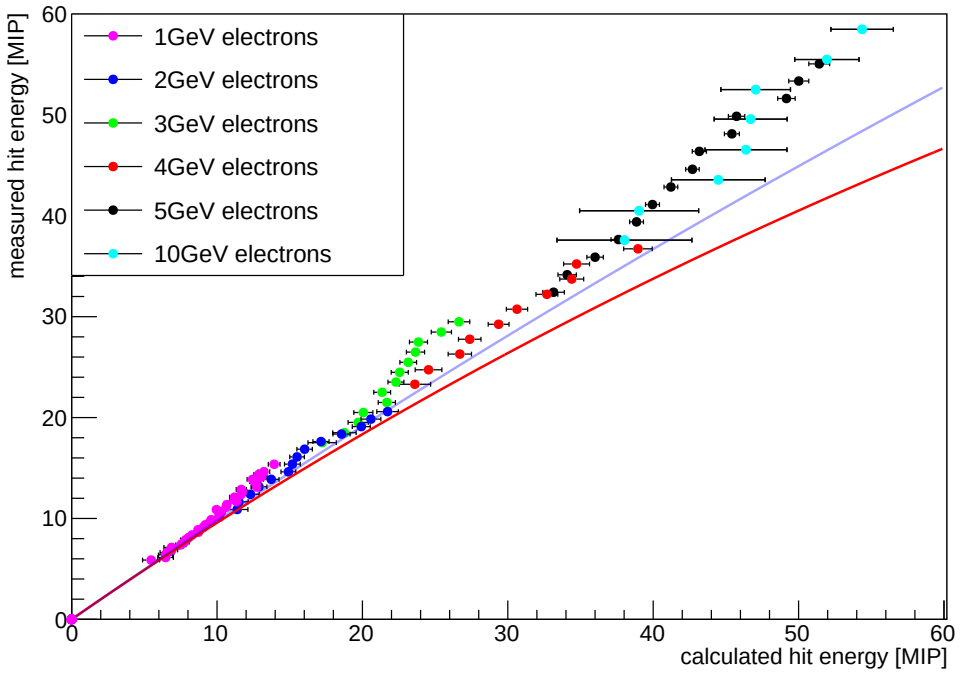

Figure 12: Correlation between the measured hit energy and calculated hit energy using the extrapolated energy sum for the cluster hit energy The lines are the saturation curves for:
blue: number of effective pixels = 2 × number of pixels
red: number of effective pixels = number of pixels

5. Conclusion

Saturation curves are an important input when reconstructing the number of incident photons from SiPM measurements. For highly granular calorimeters it would be desirable to extract them from beam data to avoid a separate SiPM measurement setup..
Different methods to extract saturation curves have been investigated for electron beam data with energies between 1GeV and 20GeV, taken with an AHCAL prototype. The AHCAL is a steel-scintillator sampling calorimeter which is read out by SiPMs.
The actual hit energy is determined by using the sum of all measured hit energies E_{sum} as reference. To obtain the actual hit energy the correct reference energy has to be chosen.
It was observed that the positive correlation between hit energy and energy sum needs to be taken into account. However in doing so, no independent reference energy could be identified. No saturation can be observed.
For ongoing studies these challenges need to be accounted for. However, in light of these results an external setup may be preferable.

A. Appendix

layer	number of pixels
1-6	2668
7	1600
8-15	1300

Table 1: Number of pixels in the SiPMs. Layer 1-6, layer 7 layer 8-15 used each the same SiPMs

beam energy	layer	x-position	y-position	slice width [MIP]
1GeV	4	12	13	0,25
2GeV	6	12	13	0,75
3GeV	6	12	13	1
4GeV	6	12	13	1,5
5GeV	6	12	13	1,75
10GeV	7	13	13	2
20GeV	7	13	13	2,25

Table 2: Selected tiles for different beam energies.
The first 6 layers obtain the same SiPMs with trenches. Layer 7 obtains similar ones with trenches as well. From layer 8 on the SiPMs are without trenches.

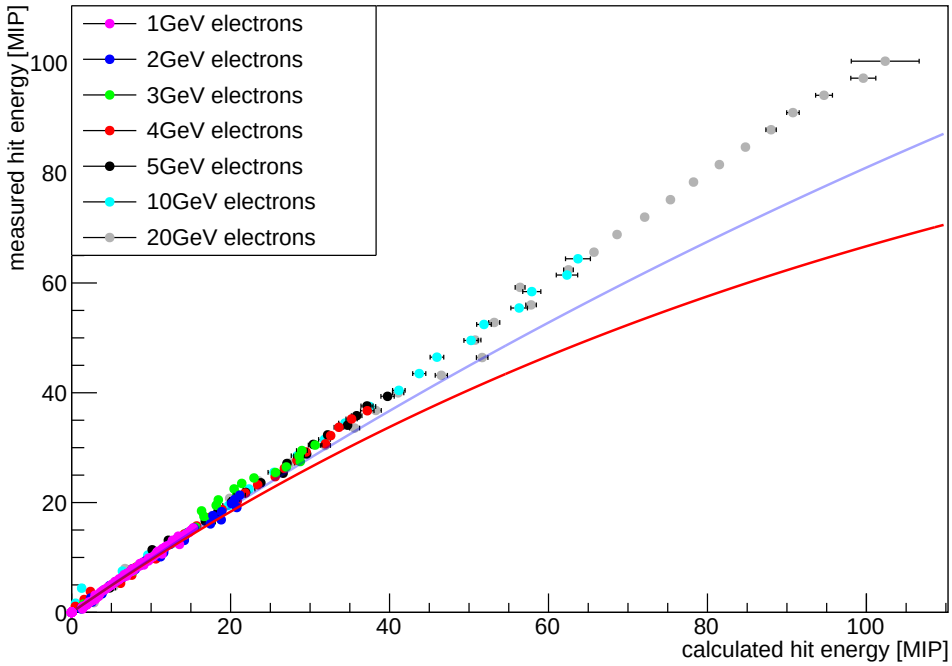

Figure 13: saturation curves for all beam energies with hit energy dependent reference energy.
The lines are the saturation curves for:
blue: number of effective pixels = 2 × number of pixels
red: number of effective pixels = number of pixels

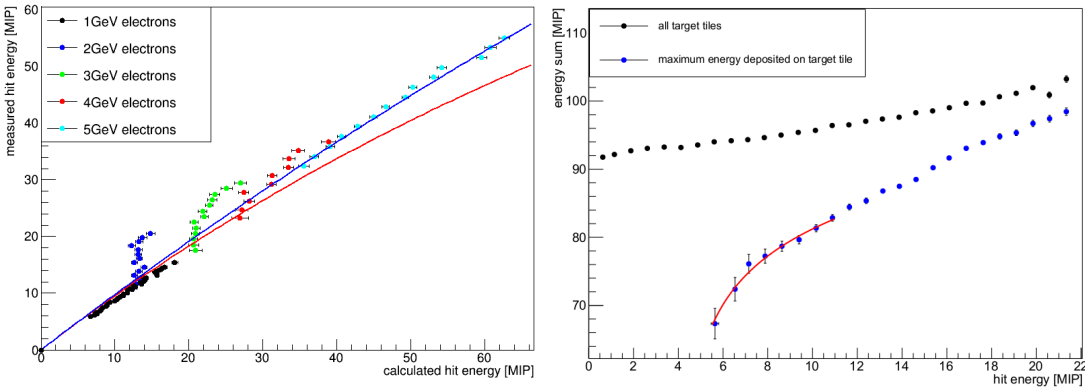

(a) Saturation curves for all beam energies with extrapolated energy sum as reference energy.

(b) Correlation curve between E_{sum} and E_{hit} for 2 GeV. The fit for a small E_{hit} range leads in this case to too small extrapolated values for E_{sum}. This explains the 2GeV curve in figure on the left.

Figure 14: Using the extrapolated energy sum as reference energy.

References

[1] Scintillator Calorimeters for a Future Linear Collider Experiment *PhD thesis O. Hartbich 2016 Wuppertal*

[2] CC BY-SA 3.0, https://commons.wikimedia.org/w/index.php?curid=22886133 *ILC Comms - Eigenes Werk*

[3] Electromagnetic Cascade, *http://hardhack.org.au/book/export/html/76*

[4] Design and Calibration of Scintillator Tiles and SiPMs for the AHCAL *talk 2016, Morioka, Japan D. Lomidze, et al. 2016*